IOP Conf. Series: Materials Science and Engineering **444** (2018) 082019 doi:10.1088/1757-899X/444/8/082019

The optimal design of a 3D pentagonal toroid with circular cross-section used in manufacturing of LPG storage tanks

M Țălu[1], M Bică[1] and Ș Țălu[2]

[1]Department of Applied Mechanics and Civil Engineering, Faculty of Mechanics, University of Craiova, Dolj county, Romania
[2]The Directorate of Research, Development and Innovation Management (DMCDI), Technical University of Cluj-Napoca, Cluj county, Romania

E-mail: marinbica52@gmail.com

Abstract. This paper presents a 3D solid modelling to generate a pentagonal toroid with circular cross-section used in manufacturing of LPG storage tanks from the automotive industry. Stress and linear deformation analysis are applied to optimize the geometrical product shape. As a result, in numerical simulation a feasible time-cost integrated project schedule was developed to formulate a construction sequence of product components based on the physical relationships between CAD objects.

1. Introduction

In manufacturing of storage fuel tanks in automotive industry various models, options and changes in trends offered by the materials were used in a wide-ranging during the last few decades to satisfy the demands of the competitive market for new models and materials [1-6].

Virtual CAE (computer aided engineering) tools play an important role in 3D designing geometrical solutions in storage fuel tanks used in automotive industry. The ability to combine advanced materials and material states allow developing new manufacturing strategies [7-9].

Various research teams have attempted to develop innovative ways in 3D CAD modelling of prototypes of storage fuel tanks, through continuous innovation into the designing process based on the cost and performance [10, 11].

Both static and dynamic conditions are combined in 3D CAD design of storage fuel tanks for selection of materials that offer advantages (high specific strength, low cost, good forming characteristics, high impact resistance and thermal stability) that give the optimum efficiency in terms of structure, service life and durability [12-17]. This information is shown to be essential in geometric pre-processing phases for finite element analysis (FEA) purposes.

In order to meet these requirements, in recent 3D models, computational analysis and mechanical tests were made to determine various related factors of design engineering to satisfy the general structural design and certification rules and decrease fabrication costs.

2. Design methodology

Let's consider the 3D model generated by revolving of a generating circle C_G along a guiding pentagonal curve C_D, with connected round corners, as shown in figure 1.

(a) (b) (c)

Figure 1. The axonometric representation of the parametric 3D solid model.

These 3D pentagonal toroids with circular cross-section have two symmetry planes: one horizontal and one vertical, to define the locations of important geometrical features, as shown in figure 2.

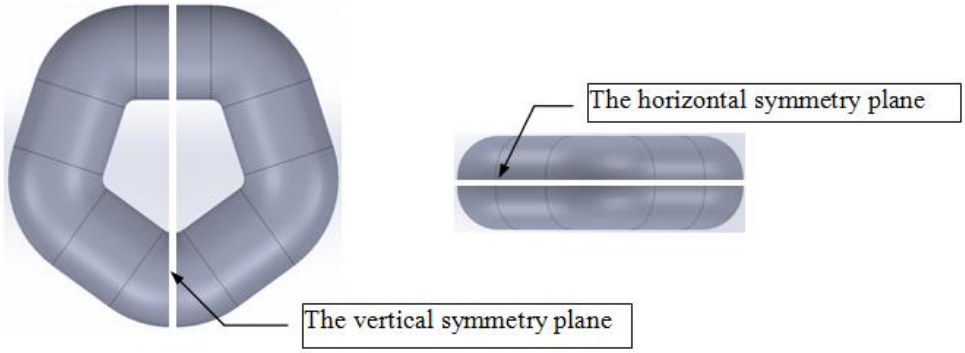

(a) (b)

Figure 2. The symmetry planes of the 3D toroidal solid: (a) the vertical plane; (b) the horizontal plane.

The following parameters were applied as input parameters to the 3D parametric model (figure 3): a) a generating circle with a radius R = 200 mm, and b) the guiding curve C_D, a pentagon with a side value L = 400 mm, which is connected to corners with a radius R = 250 mm.

Different isometric views of the parametric 3D model are shown in figure 3.

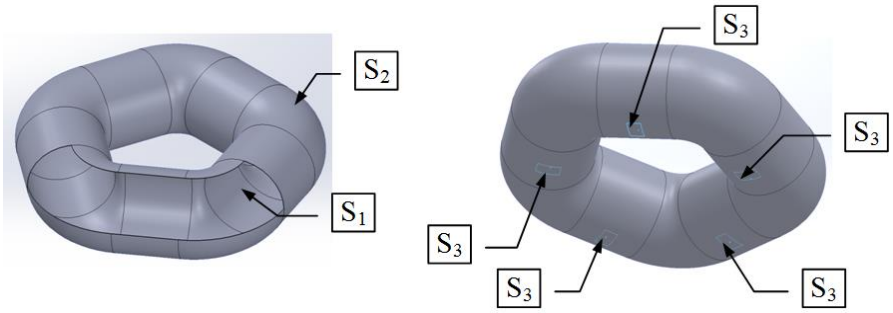

(a) (b)

Figure 3. Different isometric views of the 3D toroidal solid.

Optimized CAD design of these fuel storage tanks was imported to SolidWorks 2018 software for analysis with the: Static, Thermal and Design Study modules.

The parameterized model used in the numerical simulation is shown in figure 3 and the notations are specified in the surfaces where are applied the loads and restrictions. The design data used are:

- the tank material is AISI 4340 steel;

- the maximum hydraulic test pressure: p_{max} = 30 bar, applied on surface S_1;
- the working temperature between the limits: t = -30 °C up to t = 60 °C, applied on surface S_2;
- five supporting surfaces located on the inferior side (applied on surface S_3);
- the duration of the tank exploitation: n_a = 20 years;
- the corrosion rate of the material: v_c = 0.085 mm/years.

The applied optimization function is intended to achieve a minimum mass.

The calculation had a mesh standard type, solid mesh with high quality, automatic transition, Jacobian in 16 points, maximum element size 20 mm, tolerance 0.5 mm, number of nodes 130864, number of elements 65579, maximum aspect ratio 19.48, number of degrees freedom 344787.

The applied restriction of constraint is that the value of Von Mises effort $\sigma_{rez} \leq \sigma_a$ = 710 N/mm^2 (σ_a - the admissible value of the traction stress of the material). Applying the optimization procedure, the obtained values are: the thickness s = 2.7 mm for t = -30 °C with the stress value of the $\sigma_{rez.\,max}$ = 707.825 N/mm^2 and linear deformation value u_{max} = 1.106 mm.

Distributions of the state of stress and of linear deformations are shown in fig. 4.

It can be noted that the highest values of efforts in the 3D model occur in the pentagonal inner connection zones (as shown in fig. 4a), while the maximum deformations occur on the upper part of the model, where the deformation of the tank cover is not influenced by the tank support surfaces (which are considered fixed, as shown in fig. 4b).

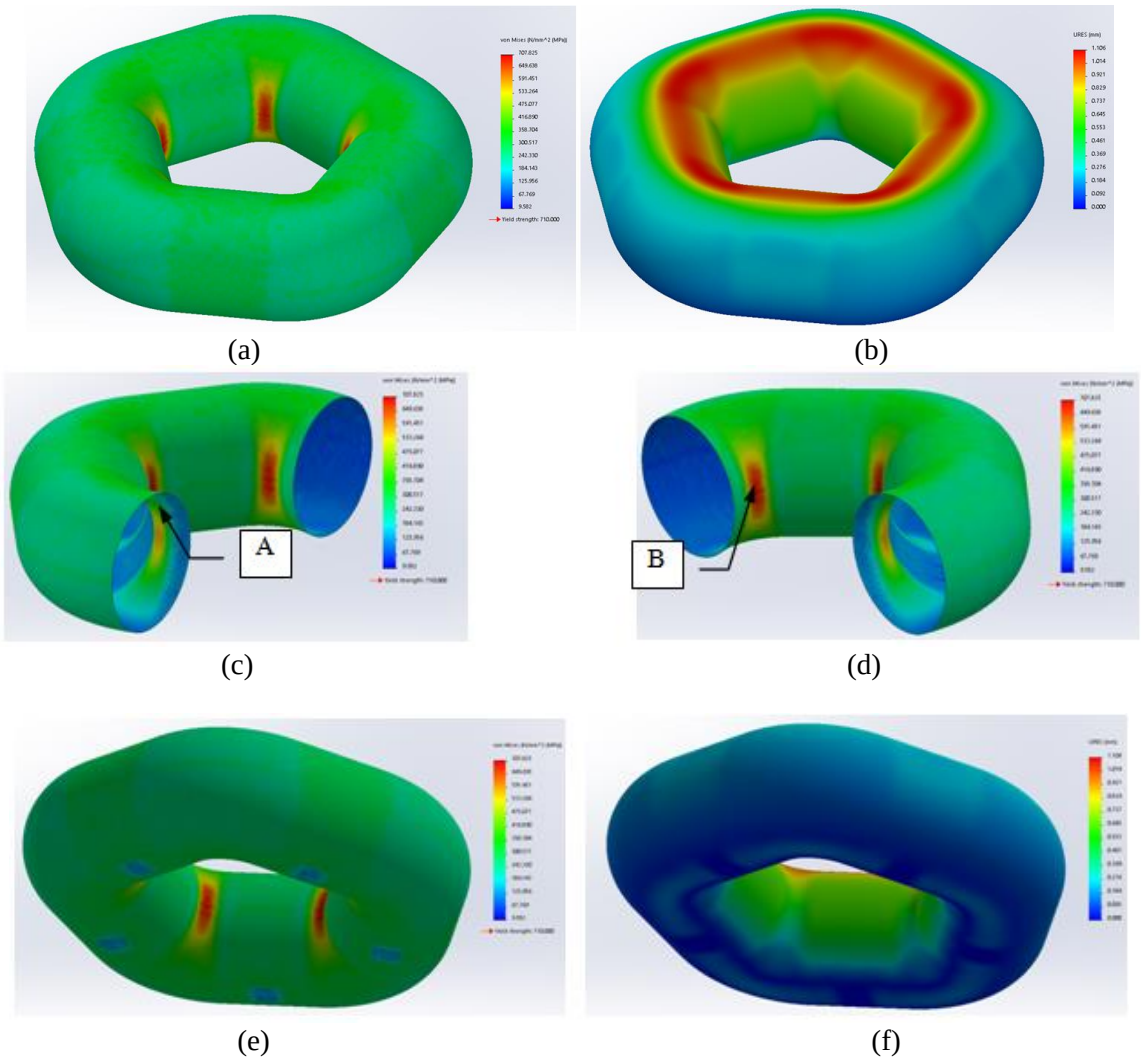

(a) (b) (c) (d) (e) (f)

Figure 4. Distributions of the state of stress and of linear deformations of the parametric 3D model.

Distributions of the state of stress and of linear deformations for different temperatures: a1 & b1) t = -30 °C, a2 & b2) t = 0 °C, a3 & b3) t = 30 °C and a4 & b4) t = 60 °C) are shown in figure 5.

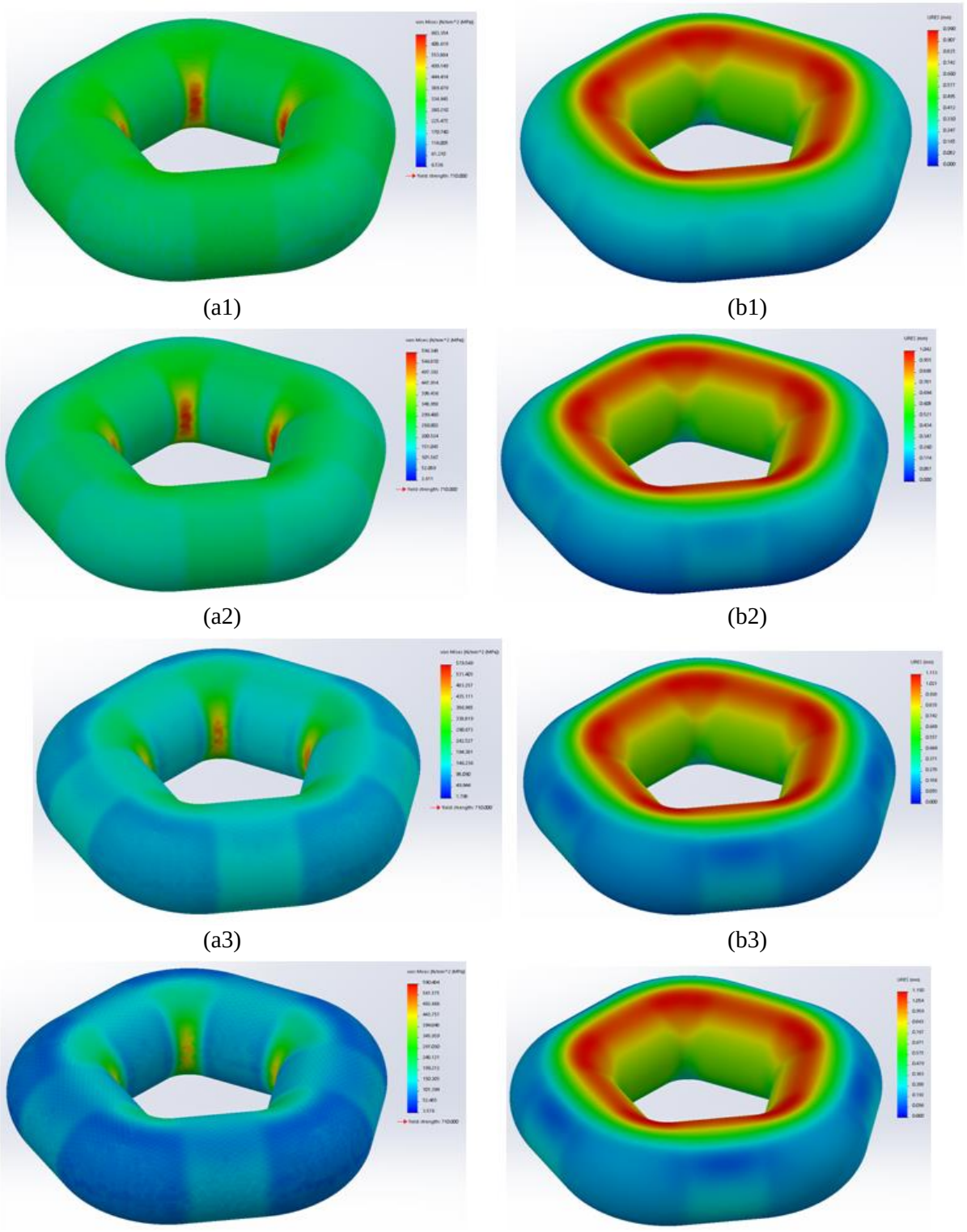

(a1) (b1)

(a2) (b2)

(a3) (b3)

(a4) (b4)

Figure 5. Distributions of the state of stress and of the linear deformations for different temperatures: a1 & b1) t = -30 °C, a2 & b2) t = 0 °C, a3 & b3) t = 30 °C and a4 & b4) t = 60 °C).

The graphs of the 3D variation of: a) the Von Mises stress variation (fig. 6a), b) and the resulting linear deformations variation (fig. 6b) are given in dependency with the temperature and the evolution of corrosion wear occurring during the exploitation.

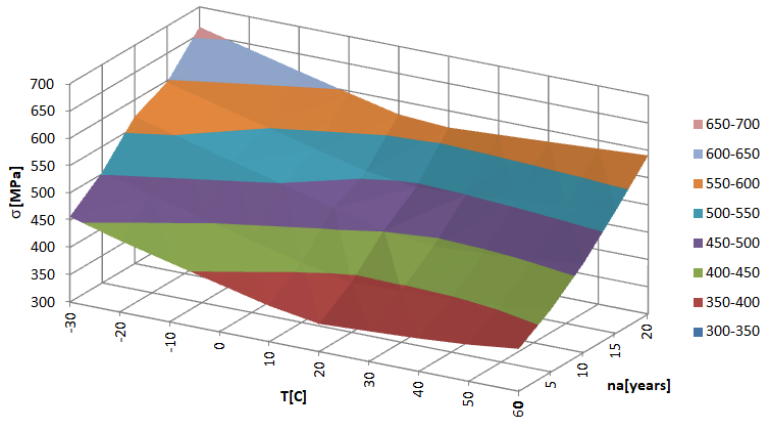

(a)

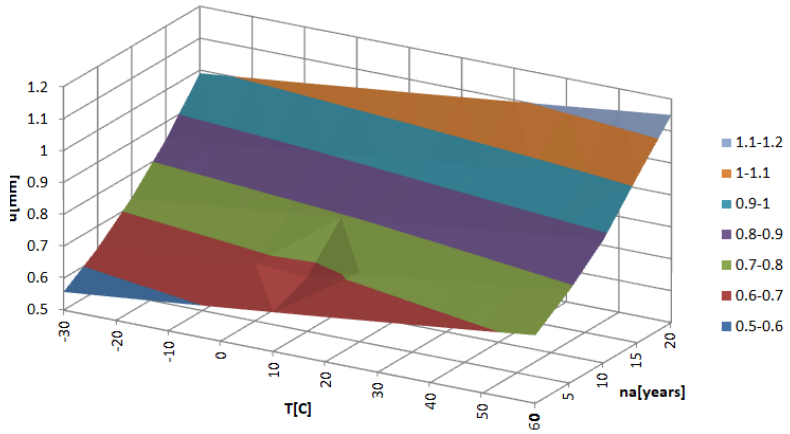

(b)

Figure 6. Distributions of: (a) the Von Mises stress variation and (b) the resulting linear deformations variation in dependency with the temperature and n_a.

The formula for calculating the thickness is the following:

$$s_{real} = s_{opt} + v_c \cdot n_a + abs(A_i) + \Delta s_a, \quad (1)$$

where: - v_c, corrosion rate of the cover, v_c = 0.085 mm/years;
- n_a, number of years of exploitation, n_a = 20 years;
- A_i, the lower deviation of the laminate sheet, A_i = - 0.6 mm, for s = 2…5 mm;
- Δs_a = 0.1 s = 0.27 mm, thinning of the sheet caused by the head cover embossing.

Finally, the minimum thickness of the sheet laminate is determined as:

$$s_{real\ min} = 2.7 + 0.085 \cdot 20 + abs(-0.6) + 0.1 \cdot 2.7 = 5.27\ mm. \quad (2)$$

A laminate sheet of AISI 4340 steel with a thickness of $s = 5.5^{+0.25}_{-0.6}$ mm is chosen for analysis.

The numerical simulation was made for n_a = 20 years which corresponds to the end of exploitation time when the cover thickness is minimal s = 2.9 mm. The variation of stress and of linear deformations with temperature and number of years of exploitation is shown in tables 1 & 2.

Table 1. The variation of stress with temperature and number of years of exploitation.

	σ, N/mm^2									
t, °C	-30	-20	-10	0	10	20	30	40	50	60
n_a = 0 years	456.3	430.9	408.8	387.0	365.5	350.7	355.3	360.2	367.1	377.6
n_a = 5 years	503.0	479.2	455.7	432.5	409.6	391.6	394.4	397.5	404.3	414.6
n_a = 10 years	569.4	545.3	521.4	497.8	474.3	451.2	440.9	445.4	453.6	463.4
n_a = 15 years	597.2	574.0	551.1	528.7	506.7	495.3	500.3	507.3	515.8	524.6
n_a = 20 years	663.3	640.6	618.2	596.3	575.3	569.4	574.3	579.5	584.9	590.4

Table 2. The variation of linear deformations with temperature and number of years of exploitation.

	u, mm									
t, °C	-30	-20	-10	0	10	20	30	40	50	60
n_a = 0 years	0.557	0.573	0.589	0.606	0.623	0.640	0.658	0.676	0.694	0.713
n_a = 5 years	0.631	0.647	0.663	0.680	0.67	0.715	0.733	0.752	0.771	0.79
n_a = 10 years	0.726	0.742	0.759	0.776	0.794	0.812	0.830	0.848	0.867	0.885
n_a = 15 years	0.845	0.863	0.881	0.90	0.919	0.938	0.958	0.978	0.998	1.02
n_a = 20 years	0.990	1.007	1.024	1.042	1.059	1.077	1.095	1.113	1.132	1.15

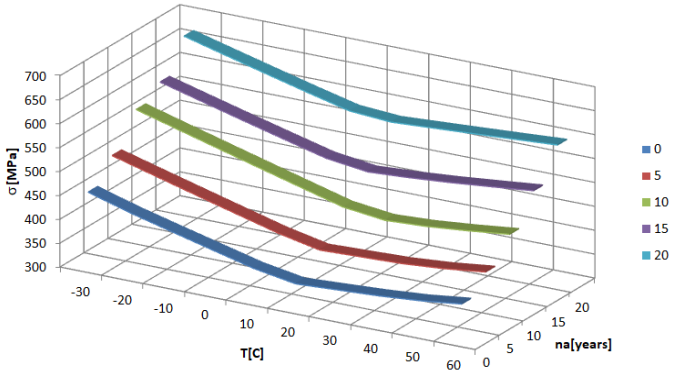

(a)

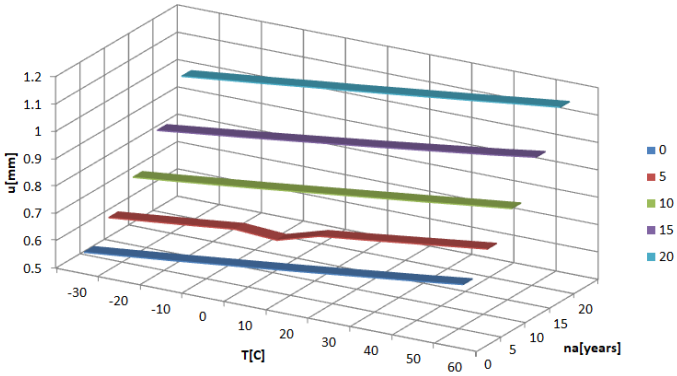

(b)

Figure 7. Distributions of: (a) the Von Mises stress variation and (b) the resulting linear deformations variation for n_a = 0, 5, 10, 15 and 20 years of exploitation.

The evolution of Von Mises stress variation (fig. 7a) and of the resulting linear deformations variation (fig. 7b) during the years of exploitation for n_a = 0, 5, 10, 15 and 20 years are given in figure 7.

The graphs and the variation laws determined by a polynomial interpolation of Von Mises stress variation (fig. 8a) and of the resulting linear deformations (fig. 8b) are shown in fig. 8.

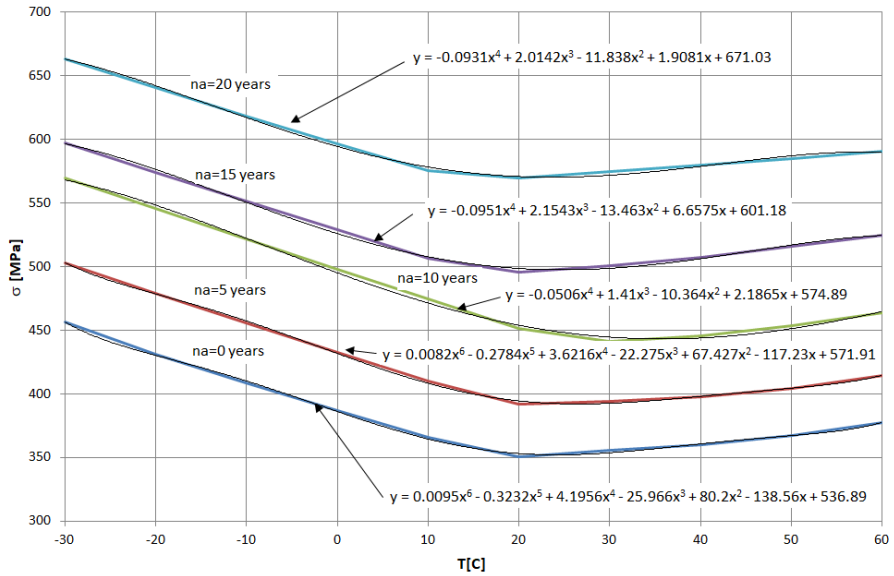

(a)

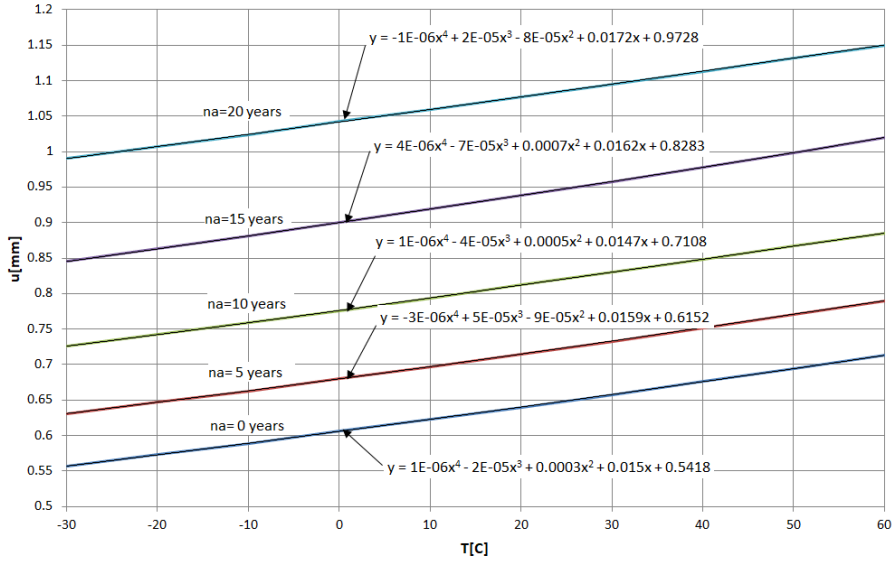

(b)

Figure 8. The graphs and the variation laws by a polynomial interpolation of: (a) the Von Mises stress variation and (b) the resulting linear deformations variation for n_a = 0, 5, 10, 15 and 20 years.

3. Conclusions

The values of Von Mises stress have minimum values between t = 20 °C and t = 30 °C, for the variation curves corresponding to n_a years of exploitation: 0, 5, 10, 15 and 20 years, having the maximum values for t = -30 °C. For t = 60 °C the values of Von Mises stress have values in the range of 81.38% to 89.01% from the maximum effort value (according fig. 8b and Table 1). Also, it can be seen that the resulting linear deformation increases with the temperature increase (fig. 8b). With the evolution of corrosion, the Von Mises stress and the resulting linear deformations increase

simultaneously. The proposed parametric modelling method of the pentagonal toroid with circular cross-section of LPG fuel tanks in automotive industry allows the determination of optimal geometric dimensions that satisfy the general structural design and certification rules.

4. References

[1] Ghiţă M C, Micu A C, Ţălu M, Ţălu Ş and Adam E 2013 Computer-Aided Design of a classical cylinder gas tank for the automotive industry *Annals of Faculty of Engineering Hunedoara - International Journal of Engineering, Hunedoara* **XI** pp 59-64

[2] Ghiţă M C, Micu A C, Ţălu M and Ţălu Ş 2013 3D modelling of a gas tank with reversed end up covers for automotive industry *Annals of Faculty of Engineering Hunedoara - International Journal of Engineering, Hunedoara* **XI** pp 195-200

[3] Ghiţă M C, Micu A C, Ţălu M and Ţălu Ş 2013 3D modelling of a shrink fitted concave ended cylindrical tank for automotive industry *Acta Technica Corviniensis – Bulletin of Engineering, Hunedoara* **VI** pp 87-92

[4] Ghiţă M C, Micu A C, Ţălu M and Ţălu Ş 2012 Shape optimization of a thoroidal methane gas tank for automotive industry *Annals of Faculty of Engineering Hunedoara - International Journal of Engineering, Hunedoara* **X** pp 295-297

[5] Ghiţă M C, Ghiţă C Ş, Ţălu Ş and Rotaru S 2014 Optimal design of cylindrical rings used for the shrinkage of vehicle tanks for compressed natural gas *Annals of Faculty of Engineering Hunedoara - International Journal of Engineering, Hunedoara* **XII** pp 243-250

[6] Ghiţă M C, Micu A C, Ţălu M and Ţălu Ş 2012 Shape optimization of vehicle's methane gas tank *Annals of Faculty of Engineering Hunedoara - International Journal of Engineering, Hunedoara* **X** pp 259-266

[7] Bică M, Ţălu M and Ţălu Ş 2017 Optimal shapes of the cylindrical pressurized fuel tanks *Magazine of Hydraulics, Pneumatics, Tribology, Ecology, Sensorics, Mechatronics (HIDRAULICA)* **4** pp 6-17

[8] Ţălu Ş, Ţălu M 2017 The influence of deviation from circularity on the stress of a pressurized fuel cylindrical tank *Magazine of Hydraulics, Pneumatics, Tribology, Ecology, Sensorics, Mechatronics (HIDRAULICA)* **4** pp 34-45

[9] Vintilă D, Ţălu M, Ţălu Ş 2017 The CAD analyses of a torospheric head cover of a pressurized cylindrical fuel tank after the crash test *Magazine of Hydraulics, Pneumatics, Tribology, Ecology, Sensorics, Mechatronics (HIDRAULICA)* **4** pp 57-66

[10] Ţălu M, 2017 The influence of the corrosion and temperature on the Von Mises stress in the lateral cover of a pressurized fuel tank *Magazine of Hydraulics, Pneumatics, Tribology, Ecology, Sensorics, Mechatronics (HIDRAULICA)* **4** pp 89-97

[11] Ţălu M, Ţălu Ş 2018 Analysis of temperature resistance of pressurized cylindrical fuel tanks *Magazine of Hydraulics, Pneumatics, Tribology, Ecology, Sensorics, Mechatronics (HIDRAULICA)* **1** pp 6-15

[12] Ţălu Ş and Ţălu M 2010 CAD generating of 3D supershapes in different coordinate systems *Annals of Faculty of Engineering Hunedoara - International Journal of Engineering, Hunedoara* **VIII** pp 215-219

[13] Ţălu Ş and Ţălu M 2010 A CAD study on generating of 2D supershapes in different coordinate systems *Annals of Faculty of Engineering Hunedoara - International Journal of Engineering, Hunedoara* **VIII** pp 201-203

[14] Ţălu Ş 2015 *Micro and nanoscale characterization of three dimensional surfaces. Basics and applications* (Cluj-Napoca: Napoca Star Publishing House)

[15] Niţulescu T. and Ţălu Ş 2001 *Applications of descriptive geometry and computer aided design in engineering graphics* (Cluj-Napoca: Risoprint Publishing house)

[16] Ţălu Ş and Ţălu M 2007 *AutoCAD 2006. Three-dimensional designing* (Cluj-Napoca: MEGA Publishing house)

[17] Ţălu Ş 2017 *AutoCAD 2017* (Cluj-Napoca: Napoca Star Publishing house)